

Rac1 and Rac3 GTPases Control Synergistically the Development of Cortical and Hippocampal GABAergic Interneurons

Valentina Vaghi¹, Roberta Pennucci¹, Francesca Talpo², Sara Corbetta¹, Valentina Montinaro¹, Cinzia Barone¹, Laura Croci¹, Paolo Spaiardi², G. Giacomo Consalez¹, Gerardo Biella² and Ivan de Curtis^{1,3}

¹Division of Neuroscience, San Raffaele Scientific Institute, 20132 Milan, Italy, ²Department of Biology and Biotechnology “L. Spallanzani”, Università di Pavia, 27100 Pavia, Italy and ³Università Vita-Salute San Raffaele, 20132 Milan, Italy

Address correspondence to Prof. Ivan de Curtis, Division of Neuroscience, San Raffaele Scientific Institute, Via Olgettina 58, 20132 Milano, Italy. Email: decurtis.ivan@hsr.it

The intracellular mechanisms driving postmitotic development of cortical γ -aminobutyric acid (GABA)ergic interneurons are poorly understood. We have addressed the function of Rac GTPases in cortical and hippocampal interneuron development. Developing neurons express both *Rac1* and *Rac3*. Previous work has shown that *Rac1* ablation does not affect the development of migrating cortical interneurons. Analysis of mice with double deletion of *Rac1* and *Rac3* shows that these GTPases are required during postmitotic interneuron development. The number of parvalbumin-positive cells was affected in the hippocampus and cortex of double knockout mice. Rac depletion also influences the maturation of interneurons that reach their destination, with reduction of inhibitory synapses in both hippocampal CA1 and cortical pyramidal cells. The decreased number of cortical migrating interneurons and their altered morphology indicate a role of *Rac1* and *Rac3* in regulating the motility of cortical interneurons, thus interfering with their final localization. While electrophysiological passive and active properties of pyramidal neurons including membrane capacity, resting potential, and spike amplitude and duration were normal, these cells showed reduced spontaneous inhibitory currents and increased excitability. Our results show that *Rac1* and *Rac3* contribute synergistically to postmitotic development of specific populations of GABAergic cells, suggesting that these proteins regulate their migration and differentiation.

Keywords: cortex, GABAergic interneurons, hippocampus, neuronal migration, Rac GTPases

Introduction

Inhibitory γ -aminobutyric acid (GABA)ergic interneurons play fundamental roles in modulating neuronal circuits (Batista-Brito and Fishell 2009; Gelman and Marín 2010). The abnormal development of these cells may alter the balance between excitatory and inhibitory activities that is required for proper brain function. Such an unbalance is believed to be at the basis of intellectual and developmental disabilities such as epilepsy, autism, and schizophrenia (Brooks-Kayal 2011). Most of the cortical and hippocampal GABAergic cells are born in the medial (MGE) and caudal (CGE) ganglionic eminences of the ventral telencephalon (Wonders and Anderson 2006). After birth, the precursors migrate tangentially from their site of origin, toward their final destination either in the cortex or in the hippocampus (Nadarajah et al. 2002; Ang et al. 2003; Tanaka et al. 2006). After reaching the cortex through 1 of 3 migratory streams along the marginal zone (MZ), the subplate, or the subventricular zone (SVZ), the interneurons adopt a radial trajectory within the cortical plate

(CP) to properly distribute throughout the different cortical layers (Hernández-Miranda et al. 2010).

Several transcription factors and a number of extracellular cues that drive the migration and differentiation of the cortical and hippocampal GABAergic cells have been identified (Hernández-Miranda et al. 2010). On the other hand, very little is known about the intracellular mechanisms that drive the different phases of interneuron development. Rho GTPases are important regulators of cytoskeletal dynamics. Among them, Rac proteins are critical in several aspects of neuronal development (de Curtis 2008). Previous studies addressing the role of Rac1 in the development of cortical interneurons suggested that Rac1 was not directly implicated in regulating the development of postmitotic migrating interneurons (Chen et al. 2007; Vidaki et al. 2012). On the other hand, vertebrates express also the neural-specific Rac1B/Rac3 GTPase (Haataja et al. 1997; Malosio et al. 1997; Albertinazzi et al. 1998, 2003) that is specifically expressed in the developing mouse peripheral and central neurons (Corbetta et al. 2005). The expression of Rac3 is developmentally regulated, with a peak at time of intense neurite branching and synaptogenesis (Bolis et al. 2003), and a pattern of expression that is often but not always overlapping with that of Rac1 (Corbetta et al. 2005).

We have generated 3 mutant mouse lines: Rac3^{KO} mice (Corbetta et al. 2005); conditional knockout (KO) for Rac1 (Rac1^N) obtained by crossing Rac1^{fl^{ox}/fl^{ox}} (Walmsley et al. 2003) with Synapsin-I-Cre (SynI-Cre) mice (Zhu et al. 2001) to delete Rac1 in postmitotic developing neurons; and double KO mice (Rac1^N/Rac3^{KO}) obtained by the combination of the previous 2 lines. The double KO mice are neurologically impaired and show spontaneous epileptic seizures, with lethality around the end of the second postnatal week (Corbetta et al. 2009). In this study, we show that Rac1 and Rac3 contribute synergistically to the development of cortical and hippocampal GABAergic interneurons, suggesting the implication of these GTPases in their migration and differentiation. The electrophysiological analysis indicates a possible correlation between the loss of GABAergic interneurons and the epileptic phenotype detected in Rac1/Rac3 double mutant mice.

Materials and Methods

Mice

Experimental handling of mice was in accordance with institutional guidelines and EEC regulation n. 86/609/CEE. All transgenic lines used in this study including KO carrying single or double mutation of

the genes for Rac1 and Rac3 GTPases (Walmsley et al. 2003; Corbetta et al. 2005, 2009), SynI-Cre transgenic mice specifically expressing the viral Cre recombinase under the control of the synapsin I promoter in differentiated neurons (Zhu et al. 2001), and ROSA26 mice (Soriano 1999) have been characterized previously. The genotypes were determined as described (Corbetta et al. 2009). In the experiments, controls for Rac3^{KO}, Rac1^N, and double KO mice were wild type, Rac1^{flox/flox} or Rac1^{flox/+} (indicated as Rac1^{flox}), and Rac3^{KO} littermates, respectively.

Antibodies

Antibodies included rabbit polyclonal anti-calretinin (CR), 1:1000, from Chemicon International; rabbit polyclonal anti-parvalbumin (PV), 1:2000, PV-28 from Swant; goat polyclonal anti-PV, 1:300, PVG-214 from Swant; rabbit polyclonal anti-calbindin (CB), 1:1000, CB-38a from Swant; rabbit polyclonal anti-neuronal nitric oxide synthase (nNOS), 1:2000, from Millipore; rat monoclonal anti-somatostatin (SOM), 1:200, from Chemicon International; rabbit polyclonal anti-vesicular GABA transporter (VGAT), 1:150, from Synaptic Systems; mouse monoclonal anti-glutamic acid decarboxylase 67 (GAD67), 1:100, from Chemicon International; Alexa Fluor-conjugated secondary antibodies, 1:200, from Invitrogen; biotinylated goat anti-rabbit (1:200) and rabbit anti-rat (1:100) antibodies from Vector Laboratories.

Histology, Immunohistochemistry, and Immunofluorescence

Mice were subjected to deep anesthesia and perfused with 4% paraformaldehyde. Brains were postfixed with 4% paraformaldehyde and cryoprotected before freezing, and 12–20- μ m-thick sections were stained with cresyl violet or immunostained. For immunohistochemistry, sections were incubated overnight at 4°C with primary antibodies. Primary antibodies were detected using a Vectastain Elite ABC Kit (Vector Laboratories), and sections were viewed with a Zeiss Axio-plan2 microscope with AxioCam MRC5 digital camera (Carl Zeiss MicroImaging). For immunofluorescence, primary antibodies were revealed by incubation for 1.5–2 h with Alexa Fluor-conjugated secondary antibodies and 4',6-diamidino-2-phenylindole (DAPI, Sigma-Aldrich) for nuclear staining. Sections were viewed with a Zeiss Axiovert 135 TV equipped with a QImaging Exi-Blue camera (Carl Zeiss MicroImaging). Confocal analysis was performed with a Leica TCS SP2 (Leica Microsystems).

5-Bromo-4-chloro-3-indolyl- β -D-galactopyranoside Staining

SynI-Cre mice were crossed with LacZ ROSA26 reporter mice (Soriano 1999). Brains were fixed 30 min at 4°C in 4% paraformaldehyde, and cryoprotected before freezing. For 5-bromo-4-chloro-3-indolyl- β -D-galactopyranoside (X-Gal) staining, sections were incubated either 1 h or overnight at 37°C with 5 mM K₃Fe(CN)₆, 5 mM K₄Fe(CN)₆, 2 mM MgCl₂, 0.01% sodium deoxycholate, 0.02% Nonidet P-40, 1 mg/mL X-Gal in phosphate buffer saline. After 30 min in 4% paraformaldehyde and washing in phosphate buffer saline, sections were mounted with Dako Glycerol mounting medium or further treated for immunohistochemistry.

In Situ Hybridization

In situ hybridization was performed on 20 μ m-thick mouse brain cryosections as previously described (Schaeren-Wiemers and Gerfin-Moser 1993). Probes were obtained by *in vitro* transcription of antisense and sense single-stranded RNA probes for either LIM homeobox 6 (Lhx6; Grigoriou et al. 1998) or Rac3 (Corbetta et al. 2005). Probes (0.5 μ g/mL) were incubated overnight at 56°C (for Lhx6) or 60°C (for Rac3) and revealed by incubation overnight at 4°C with anti-digoxigenin antibody (1:2000, Roche Applied Science), followed by staining with BCIP/NBT color development substrates (Roche Applied Science). For costaining, the immunostaining for PV was performed before starting the procedure for *in situ* hybridization with the probe for Rac3.

Apoptosis

Terminal deoxynucleotidyl transferase dUTP nick end labeling (TUNEL) was performed using the ApopTag® Red In Situ Apoptosis Detection Kit (Chemicon), as previously described (Pennucci et al. 2011).

Morphological Analysis and Quantification

The numbers of interneurons and Lhx6-positive cells were estimated from coronal sections. For each genotype, 7–23 sections along the rostral-caudal axis of the dorsal hippocampus and 30–50 fields from sections of the somatosensory cortex of 2–4 sets of littermates were used. CB-positive cells were quantified in 12–13 coronal sections rostral to the hippocampus from 3 sets of P0 littermates. The density of CB-positive cells was evaluated from similar areas of the SVZ or MZ using the ImageJ software (NIH Image).

We measured the length of the leading process (i.e., the longest cellular extension) and the angle of radially migrating interneurons CB-positive interneurons in the CP of P0 mice using ImageJ (Stühmer et al. 2002). For each section, a grid of virtual radial lines perpendicular to the pia was drawn, and the orientation of each cell measured in relation to the most adjacent line. Cells with an angle $\leq 25^\circ$ were considered as radially migrating (Martini et al. 2009).

For quantification of the presynaptic GABAergic terminals, the fluorescent signal of GAD67 and VGAT was evaluated in equal areas from coronal sections including comparable levels of either the CA1 stratum pyramidale, or layers IV and V of the somatosensory cortex of Rac3^{KO} and double KO mice. Laser power and settings were the same for all samples within the same experiment. Images were analyzed with ImageJ. The area occupied by fluorescent signals above the background and the mean gray value were quantified in the stratum pyramidale and in layers IV and V of the somatosensory cortex. The mean gray value is the average intensity of fluorescence per unit area. Quantitative analysis of the colocalization of PV with either VGAT or GAD67 was performed using ImageJ.

Electrophysiology

Electrophysiological experiments were performed on hippocampal and cortical slices from 18 double KO and 19 Rac3^{KO} mice (P12–P14). Transversal 350- μ m-thick slices (Stoop and Pralong 2000) were transferred to an incubation chamber filled with carboxygenated (95% O₂, 5% CO₂) artificial cerebrospinal fluid (aCSF) medium (125 mM NaCl, 2.5 mM KCl, 26 mM NaHCO₃, 15 mM Glucose, 1.3 mM MgCl₂, 2.3 mM CaCl₂, 1.25 mM NaH₂PO₄). All derivations were performed at 23–25°C on slices perfused at 0.6 mL/min with aCSF. The recording chamber was mounted on a E600FN microscope with $\times 4$ and $\times 40$ water-immersion lens (Nikon), connected to a near-infrared CCD camera. Experiments were performed on hippocampal CA1 and CA3 pyramidal neurons, or cortical layer V pyramidal neurons, by the whole-cell patch-clamp technique in voltage- and current-clamp modes. To investigate in current-clamp configuration, the spontaneous excitatory postsynaptic potentials (EPSPs) and the susceptibility to induce ictal epileptiform activity, the following intracellular solution was used: 130 mM κ -gluconate, 4 mM NaCl, 2 mM MgCl₂, 1 mM EGTA, 5 mM creatine phosphate, 2 mM Na₂ATP, 0.3 mM Na₃GTP, 10 mM HEPES-KOH, pH 7.3. To register the spontaneous inhibitory postsynaptic currents (IPSCs), pipettes were filled with 120 mM Cs-methanesulfonate, 5 mM KCl, 1 mM CaCl₂, 2 mM MgCl₂, 10 mM EGTA, 4 mM Na₂ATP, 0.3 mM Na₃GTP, 5 mM lidocaine *N*-ethylbromide, 8 mM HEPES-KOH, pH 7.3. Series resistance was always compensated by 70–90% and monitored throughout the experiment.

Recordings were made with a MultiClamp 700B amplifier with a Digidata 1322 computer interface (Molecular Devices). Data were acquired using the software Clampex 9.2 (Molecular Device), sampled at 20 kHz and filtered at 10 kHz.

Drugs were added to aCSF medium and bath perfused. Epileptiform-like discharges were induced by 50–500 μ M 4-aminopyridine (4-AP, Sigma-Aldrich), a blocker of A-type potassium channels. Spontaneous IPSCs were recorded in presence of glutamatergic synaptic blockers: 10 μ M of AMPA receptor antagonist 2,3-dioxo-6-nitro-1,2,3,

4-tetrahydrobenzo[*l*] quinoxaline-7-sulfonamide (NBQX, Tocris Cookson) and 30 μ M of the NMDA receptor antagonist 3-(2-carboxypiperazin-4-yl) propyl-1-phosphonic acid (CPP, Tocris Cookson). EPSPs were derived using 10 μ M of the GABA_A receptor antagonist bicuculline methiodide.

Data were analyzed with Clampfit 10.2 (Molecular Devices) and Origin (Microcal). For 4-AP-induced seizure-like activity, we characterized the presence of preictal events, ictal discharge, and afterdischarges. Neuronal input resistance was calculated in the linear portion of the *I*-*V* relationship during depolarizing voltage responses near the resting potential. Cell surface was estimated by integrating the capacitive current evoked by a -10-mV pulse commanded just after obtaining the whole-cell configuration.

Statistics

All graphs show means \pm SEM. Statistical significance ($P < 0.05$) was determined by Student's *t*-test.

Results

Rac1 and *Rac3* Are Required for the Development of Cortical and Hippocampal GABAergic Interneurons

Reduction in the number of PV-positive cells at different anteroposterior levels of the dorsal hippocampus of P13 mice was in average >90% in the double KO mice, 26% in *Rac1*^N, and 23% in *Rac3*^{KO} compared with corresponding controls (Fig. 1*A, C*; Supplementary Fig. S1). In the somatosensory

cortex, reduction of PV-positive cells was 75%, 15%, and 31%, respectively (Fig. 1*B, D*). PV-, SOM-, and nNOS-positive cells account for >90% of MGE-derived interneurons (Tricoire et al. 2011; Inan et al. 2012). The strong numeric reduction of GABAergic interneurons was restricted to PV-positive cells. SOM- and nNOS-positive cells from MGE and CR-positive cells from CGE were not as heavily affected in double KO mice (Fig. 1*E, F*).

The transcription factor *Lhx6* is expressed by MGE-derived cells (Danglot et al. 2006; Zhao et al. 2008) and marks PV- and a subset of SOM-positive cells (Cobos et al. 2005). The number of *Lhx6*-positive cells identified by in situ hybridization was reduced by 54% in the hippocampus and 52% in the somatosensory cortex of double KO mice (Fig. 2). As 50–60% of *Lhx6*-positive cells become PV-positive (Miyoshi et al. 2010), the decrease of PV-positive cells in double KO hippocampi may account for the reduction of most *Lhx6*-positive cells. Remaining *Lhx6*-positive cells may include SOM- and nNOS-positive cells that were only marginally affected (Fig. 1*E, F*).

Deletion of the *Rac* GTPases Causes a Defect in the Maturation of the PV-Positive Interneurons

The neurites of cortical (Fig. 3*A*) and hippocampal (data not shown) PV-positive cells were drastically reduced in double KO mice. The fluorescent signals of GABAergic presynaptic

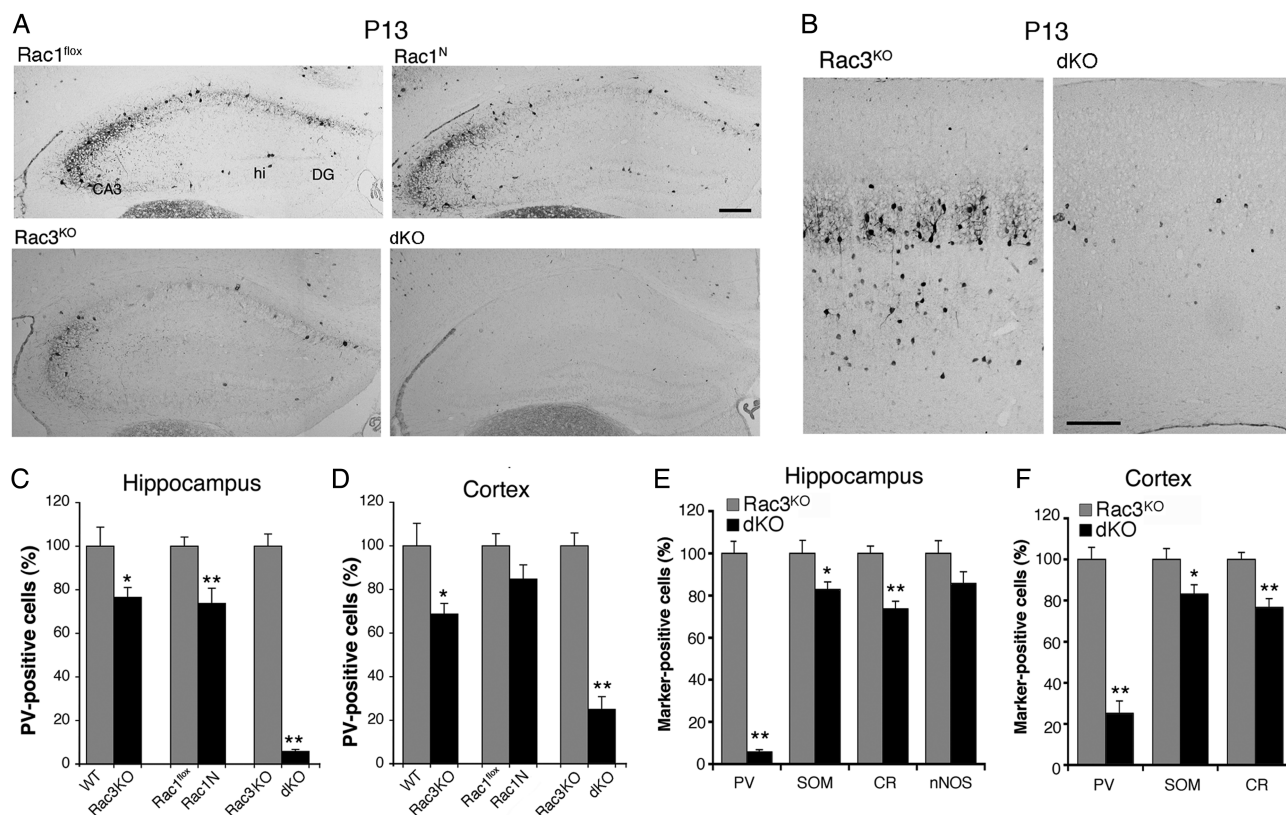


Figure 1. Double deletion of *Rac1* and *Rac3* causes the reduction of cortical and hippocampal PV-positive interneurons. (*A*) PV staining of the hippocampus of *Rac1*^{fllox}, *Rac1*^N, *Rac3*^{KO}, and double KO mice. (*B*) PV staining of the somatosensory cortex of double KO and control *Rac3*^{KO} littermates. DG, dentate gyrus; hi, hilus. Scale bars: 100 μ m. (*C*) Number of PV-positive neurons/section of hippocampus from *Rac1*^{fllox}, *Rac3*^{KO}, *Rac1*^N, and double KO mice. Graph bars are normalized means \pm SEM ($n = 7$ –16 sections from 2 to 3 mice/genotype). (*D*) Density of PV-positive neurons in the somatosensory cortex of *Rac1*^{fllox}, *Rac3*^{KO}, *Rac1*^N and double KO mice. Graph bars are normalized means \pm SEM ($n = 11$ –31 cortical fields from 2 to 3 mice/genotype). (*E* and *F*) The strong decrease in the number of interneurons is specific for the PV-positive cells. Quantification from sections of hippocampus (*E*) and somatosensory cortex (*F*) immunostained for PV, SOM, CR, or nNOS. Normalized means \pm SEM of (*E*) the number of marker-positive neurons/section ($n = 10$ –23 sections from 2 to 3 mice/genotype), and (*F*) cell density ($n = 31$ –50 cortical fields from 2 to 3 mice/genotype). * $P < 0.05$; ** $P < 0.005$.

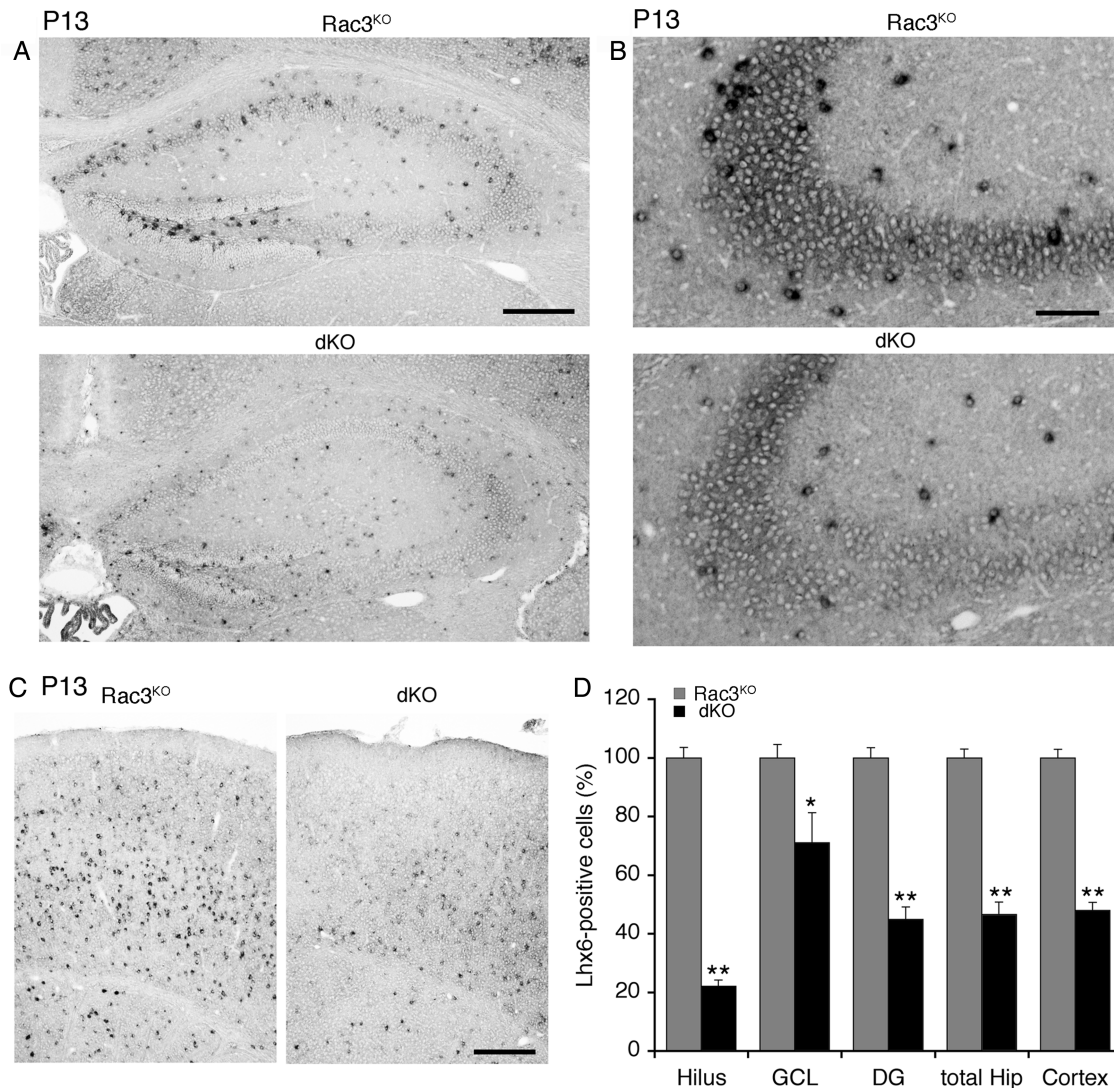


Figure 2. The number of Lhx6-positive neurons is decreased in the hippocampus and cortex of double KO mice. In situ hybridization for Lhx6 in the hippocampus (A and B) and cortex (C) of Rac3^{KO} and double KO mice. Scale bars: 300 μ m (A and C); 100 μ m (B). (D) Number of Lhx6-positive cells. Graph bars are normalized means \pm SEM ($n = 15$ sections, 3 mice/genotype). * $P < 0.05$; ** $P < 0.005$. GCL, granule cell layer; DG, dentate gyrus.

marker VGAT and of GAD67 were decreased in the stratum pyramidale of the CA1 of P13 double KO mice (Fig. 3B, D). As expected, PV was strikingly reduced (Fig. 3C). The average intensity of fluorescence per unit area (mean gray value) for GAD67 and VGAT was not altered within the marker-positive area (Fig. 3E), but the area occupied by either marker was reduced by $\approx 50\%$ (Fig. 3F). Therefore, the presynaptic input on excitatory CA1 cells was heavily reduced in double KO mice. We observed a significant decrease of the inhibitory projections of GABAergic interneurons also on cortical pyramidal neurons of layers IV and V of the somatosensory cortex (Fig. 3G, H). Together, our data show that Rac1 and Rac3 are required for the development of hippocampal and cortical inhibitory circuits.

Rac Depletion Affects the Number and Morphology of Postmitotic Migratory GABAergic Precursors

The more severe defects observed in double KO mice compared with Rac3^{KO} and Rac1^N mice suggest that Rac1 and

Rac3 are both important for the development of specific populations of cortical and hippocampal interneurons, and that the lack of either Rac may be partially compensated by the other. Rac3 has a more restricted distribution relative to Rac1, and a peak of expression during late embryonic/early postnatal development (Bolis et al. 2003). As antibodies for immunostaining of Rac3 are not available (Corbetta et al. 2005), we have used in situ hybridization (Supplementary Fig. S2A). The transcript for *Rac3* colocalized with PV immunostaining in a number of hippocampal cells (Supplementary Fig. S2B).

Immature CB-positive cells include different future interneuron subtypes, including PV-positive cells, which are first detected only in the postnatal cortex (Alcantara et al. 1996). CB-positive cells are normally used to analyze the migration of interneurons in the cortex (Anderson et al. 1997). Rac1 was found also in the developing CB-positive cortical interneurons at P0 (Supplementary Fig. S2C). We also found that the SynI-Cre transgene was active in 100% of hippocampal and in 87% of cortical PV-positive cells (Supplementary Fig. S2D–F).

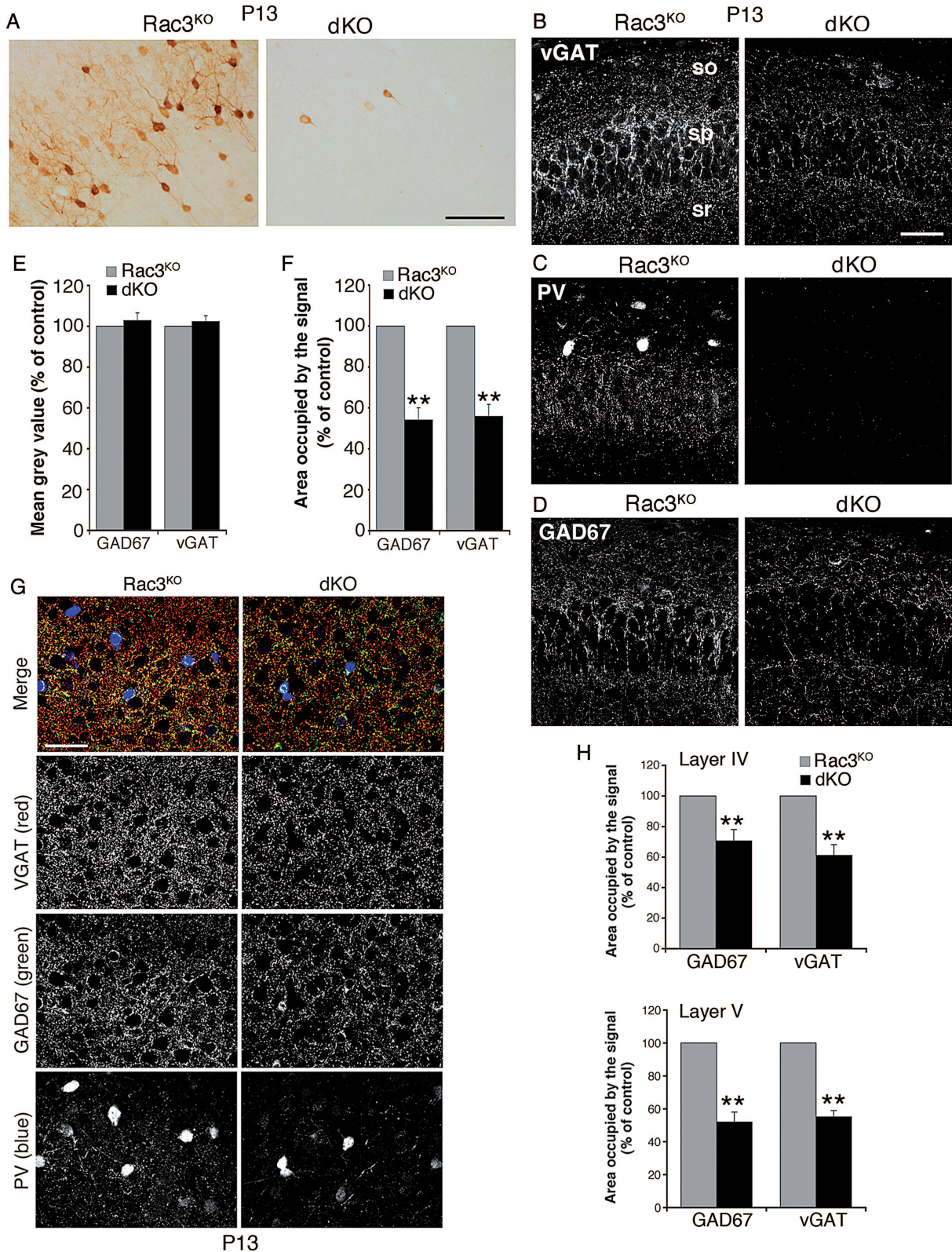


Figure 3. The inhibitory presynaptic input is reduced in the hippocampus and cortex of double KO mice. (A) PV-positive interneurons in the somatosensory cortex of P13 *Rac3*^{KO} and double KO mice. Scale bar: 100 μ m. (B–D) Confocal images of the CA1 region from P13 mice immunostained for VGAT (B), PV (C), or GAD67 (D). The inhibitory input is reduced in the stratum pyramidale of the CA1 region of double KO animals; so, stratum oriens; sp, stratum pyramidale; sr, stratum radiatum. Scale bar: 50 μ m. (E) Mean gray values, corresponding to the average intensity of fluorescence per unit area for either GAD67 or VGAT within the stratum pyramidale of CA1. Graph bars are normalized means \pm SEM (*Rac3*^{KO} = 100%; *n* = 24 CA1 fields from 3 mice/genotype). (F) Area of CA1 stratum pyramidale positive for either GAD67 or VGAT. Graph bars are normalized means \pm SEM (*Rac3*^{KO} = 100%; *n* = 24 CA1 fields from 3 mice/genotype). (G) Confocal images of layer V of the somatosensory cortex immunostained for presynaptic markers and PV. (H) Reduction of the signal for both GAD67 and VGAT in layers IV and V of the somatosensory cortex of double KO mice. Graph bars are normalized means \pm SEM (*Rac3*^{KO} = 100%; *n* = 17–20 cortical fields from 3 mice/genotype). ***P* < 0.005.

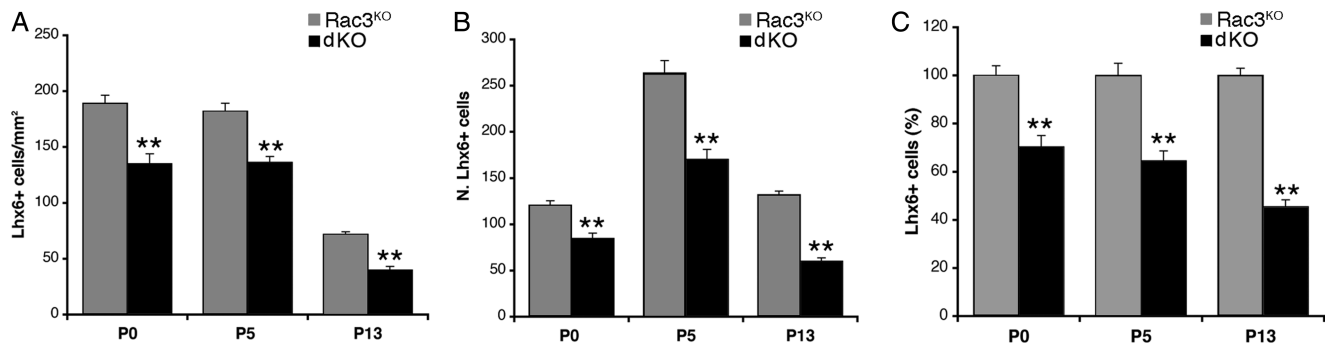


Figure 4. Quantification of Lhx6-positive cells during the postnatal development of the hippocampus. Graph bars are means \pm SEM of density (A), number/section of hippocampal hemisphere (B), and percentage (controls = 100%) (C) of Lhx6-positive cells ($n = 22$ –30 sections from 3 to 4 mice/genotype/stage). $^{***}P < 0.005$.

Therefore, Rac1 may be deleted in most cortical and hippocampal PV-positive cells.

The decrease in Lhx6-positive interneurons in the hippocampus and cortex of P13 double KO mice (Fig. 2) may be due to increased cell death and/or to the failure of these cells to reach their final destinations. The number of Lhx6-positive cells was already decreased in P5 and P0 double KO hippocampi (Fig. 4). The density of MGE-derived hippocampal interneurons peaks around birth, and sharply decreases thereafter (Tricoire et al. 2011). Accordingly, we observed a reduction of the density of hippocampal Lhx6-positive cells of Rac3^{KO} mice between P0 and P13 (Fig. 4A). The reduced density and number of Lhx6-positive cells in P0 double KO mice compared with Rac3^{KO} suggests a defect in the arrival of these cells in the hippocampus (Fig. 4A–C). Percentwise the loss of interneurons in double KO hippocampi increased from 30% (P0) to 55% (P13), suggesting an increase in cell death in the double KO hippocampi that may account for the loss of a fraction of the interneurons that have reached their final destination (Fig. 4C). In this direction, a TUNEL analysis at P0–P7 revealed a nonsignificant increase of cell death in double KO hippocampi (Rac3^{KO}: 19.1 ± 3.1 TUNEL-positive cells/section, $n = 13$; double KOs: 24.6 ± 5.6 TUNEL-positive cells/section, $n = 14$). On the other hand, cell death was undetectable in the cortex of E15.5 and E18.5 Rac3^{KO} and double KO mice (Supplementary Fig. S3A,B). In agreement with previous findings (Hevner et al. 2004), the few TUNEL-positive cells detected at P0 either in Rac3^{KO} or double KO mice did not include CB-positive interneurons (Supplementary Fig. S3C), suggesting that death of interneurons was not detectable at these stages.

We investigated a possible defect of the migratory GABAergic precursors. We first examined the time of activation of the SynI-Cre by X-Gal staining in SynI-Cre/ROSA26 embryos. SynI-Cre activity was barely detectable at E14.5, whereas it was stronger at E15.5 and later (Supplementary Fig. S4), when both tangential and radial migration of interneurons occurs (Hernández-Miranda et al. 2010). The SynI-Cre transgene was active in a significant fraction of cortical CB-positive precursors, indicating that Rac1 can be deleted in these cells (Supplementary Fig. S5). SynI-Cre was active only in a few cells of the MGE. This result indicates that deletion of both Rac GTPases in some of the mitotic progenitors may not fully account for the phenotype of the double KO mice, and supports a role of the 2 Racs during postmitotic development, after the interneurons exit from the MGE. We observed a small but significant decrease of CB-positive cells in the SVZ

migratory stream of P0 double KO mice (Fig. 5A, B), whereas no difference was observed in the MZ stream (data not shown). This is consistent with studies indicating that the SVZ is the path used by most murine cortical interneurons migrating tangentially from the MGE (Pla et al. 2006; Tanaka and Nakajima 2012).

After reaching the cortex, GABAergic interneurons switch to radial migration to properly distribute within different layers. At P0, the CB-positive cells in the CP of double KO mice had shorter leading processes ($\sim 40\%$) (Fig. 5C, D), and were more randomly oriented than Rac3^{KO} cells (Fig. 5C). The angle between the leading process and the closest virtual radial line perpendicular to the pia (Martini et al. 2009) was increased in double KO neurons (Fig. 5E), and the percentage of radially oriented neurons (with an angle $\leq 25^\circ$) decreased ($71 \pm 4.5\%$ in Rac3^{KO}; $46 \pm 6.1\%$ in double KO) (Fig. 5F). Therefore, tangential and radial migration of GABAergic precursors appears impaired in the absence of Rac1 and Rac3.

Pyramidal Neurons in Double KO Mice Show Higher Excitability and Altered Spontaneous IPSCs

The reduced number of interneurons (Fig. 1), and the consequent decrease of GABAergic input revealed in specific hippocampal and cortical areas (Fig. 3) could increase the global excitability of these brain regions. This may cause the spontaneous epileptic seizures observed in double KO mice (Corbetta et al. 2009). To test this hypothesis, we first examined the electrophysiological passive and active properties of pyramidal neurons. No differences were detected for any of the parameters measured (Table 1), with values in agreement with those described in wild-type animals (Tyzio et al. 2003). We next used the whole-cell patch-clamp technique to measure EPSPs in hippocampal pyramidal neurons from Rac3^{KO} and double KO mice (Fig. 6A). No differences were observed under basal conditions (Fig. 6B). Lower doses of 4-AP (50 μM) failed to elicit epileptiform events in either Rac3^{KO} or double KO neurons (Supplementary Fig. S6A), although we observed a significant increase in the instantaneous frequency of EPSPs in both Rac3^{KO} and double KO cells compared with basal conditions, which raised from 3.53 ± 0.66 (basal) to 6.53 ± 1.97 Hz (50 μM 4-AP) in Rac3^{KO} neurons, and from 2.08 ± 0.56 (basal) to 5.87 ± 1.34 (50 μM 4-AP) in neurons from double KO. The increase in frequency was significantly higher in double KO cells (Supplementary Fig. S6B). Application of 100 μM 4-AP elicited epileptiform

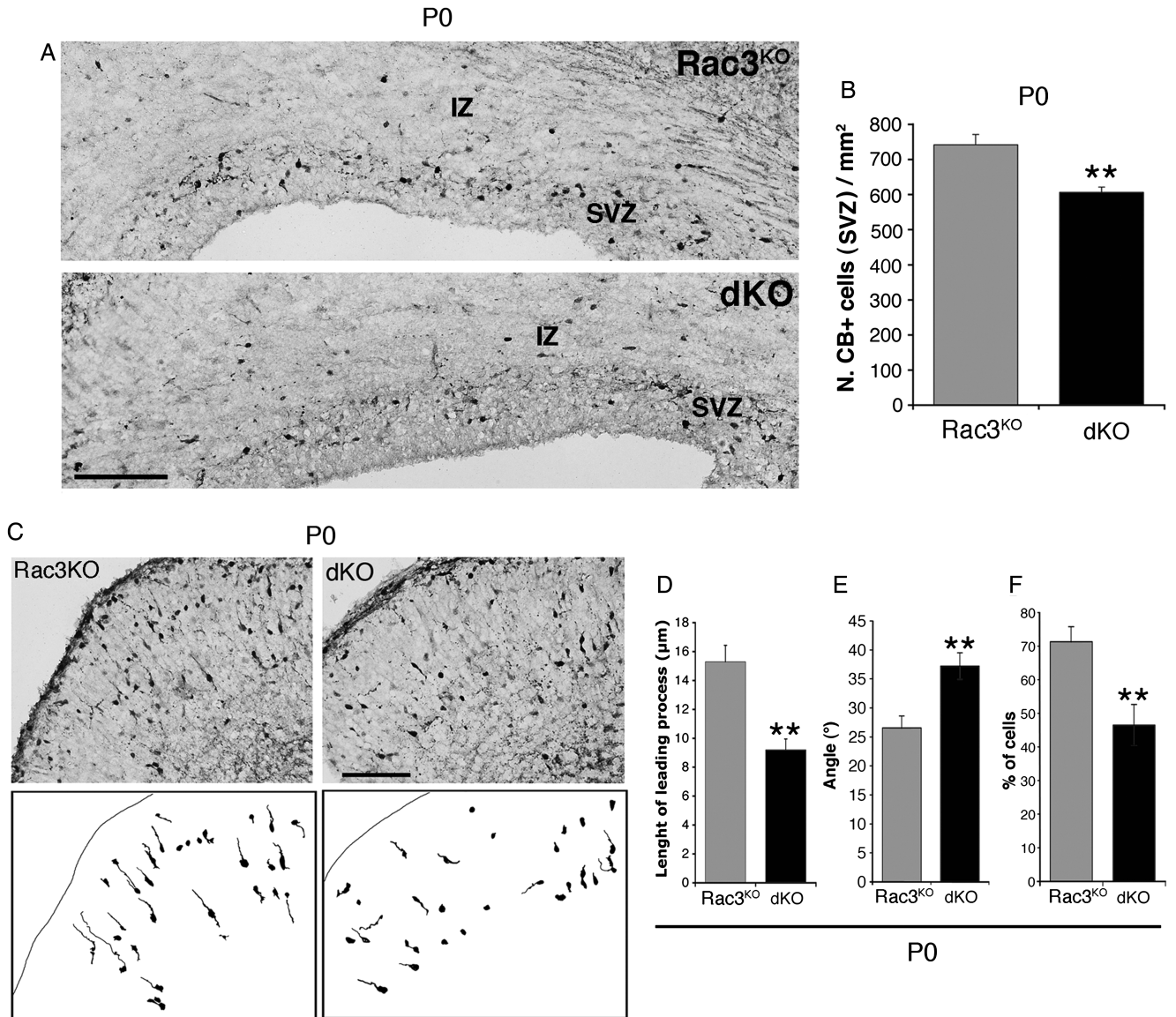


Figure 5. Number and morphology of cortical CB-positive precursors are affected in double KO mice. (A) CB-positive neurons in the SVZ migratory pathway of the cortex of P0 mice. Sections rostral to the hippocampus are shown. (B) Graph bars are means \pm SEM of the number of CB-positive cells per mm² of SVZ; $n = 18$ – 19 sections from 3 mice/genotype. $^{**}P < 0.005$. (C) Immunohistochemistry for CB in cortical sections (upper), and camera lucida from same images (lower). Scale bars: 100 μ m. (D) Length of the leading process of CB-positive cells of the CP. Graph bars are means \pm SEM ($n = 263$ control and 243 double KO cells from 3 mice/genotype). (E) Angle of CB-positive cells in the CP ($n = 145$ control and 136 double KO cells from 4 mice/genotype). (F) Percentage of CB-positive cells with an angle $\leq 25^\circ$ ($n = 13$ control and 14 double KO sections from 4 mice/genotype). $^{**}P < 0.005$.

Table 1

Passive and discharge properties measured in CA3 pyramidal neurons from control and double KO (dKO) mice.

	Capacity (pF)	I_{Na+} peak (pA)	Resting potential (mV)	Input Resistance (M Ω)	Membrane time constant (ms)	Spike Threshold (mV)	Spike amplitude (mV)	Spike duration (ms)
Control ($n = 17$)	86.1 \pm 4.1	11 224 \pm 835	-72.1 \pm 2.3	462 \pm 40	56.0 \pm 4.8	-54.2 \pm 1.5	83.0 \pm 2.7	2.0 \pm 0.1
dKO ($n = 15$)	84.6 \pm 3.6	11 084 \pm 756	-75.3 \pm 1.5	506 \pm 50	57.0 \pm 4.7	-50.8 \pm 0.8	81.8 \pm 1.9	2.0 \pm 0.1

Values are means \pm SEM. No significant differences are detected.

activity in most double KO CA3 pyramidal neurons, with a mean duration of the ictal activity of 123 ± 28 s, and with afterdischarge components detected in most cells. Ictal activity was not evoked in Rac3^{KO} perfused with 100 μ M 4-AP, although a preictal activity characterized by EPSPs with higher amplitude and frequency was observed (Fig. 6C, D).

At 500- μ M 4-AP, the ictal activity, preictal activity, and afterdischarges were elicited in 100% of Rac3^{KO} and double KO cells (Fig. 6D). Under these conditions, the time-to-ictal event (TTI), the interval between the beginning of stimulation with proconvulsant and the appearance of the ictal event, was significantly shorter in cells from double KO compared with Rac3^{KO},

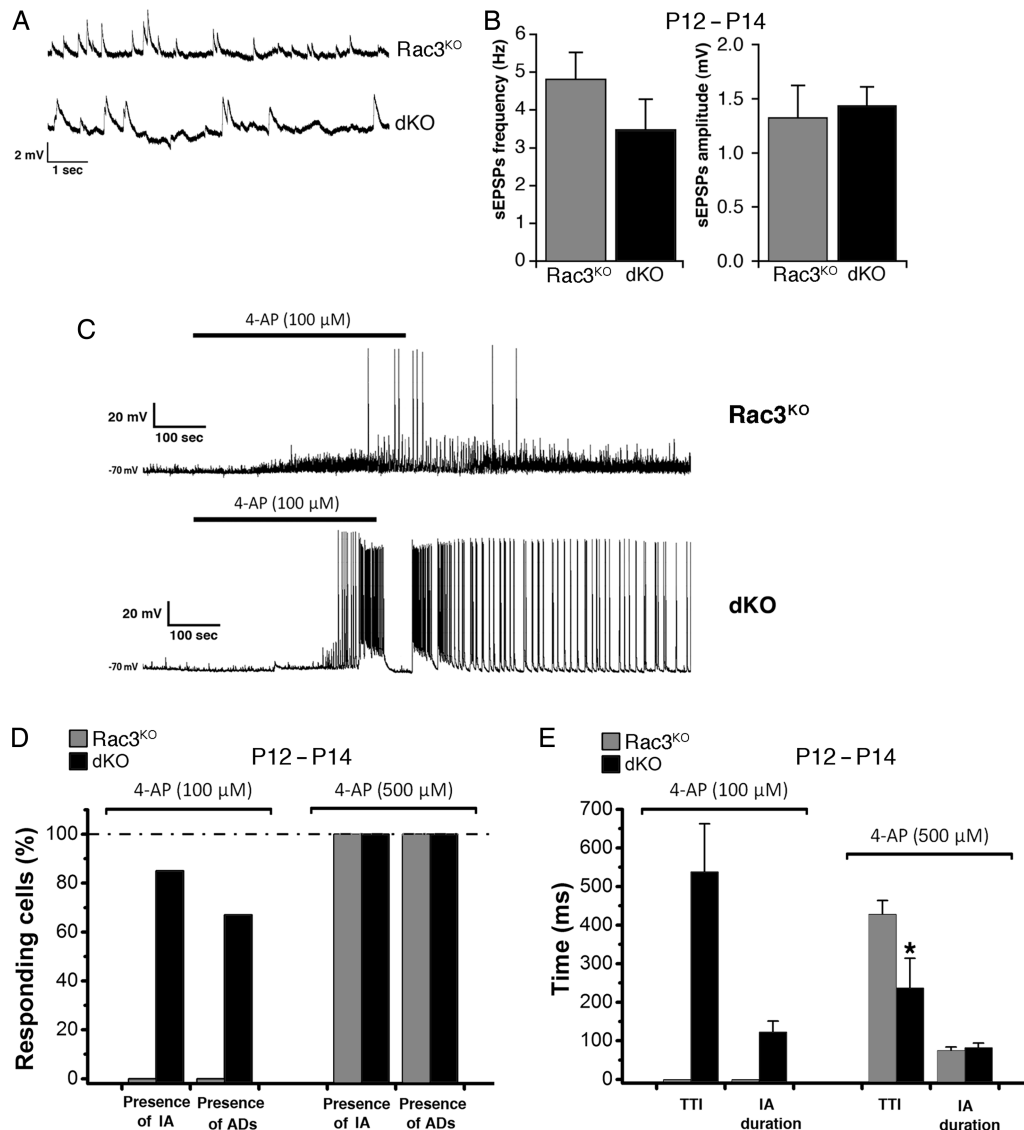


Figure 6. Rac deficiency increases hippocampal excitability and susceptibility to 4-AP-elicited epileptiform activity. (A) Spontaneous EPSPs from pyramidal cells in slices prepared from Rac3^{KO} and double KO mice. (B) Quantification revealed no differences in the instantaneous frequency and amplitude of spontaneous EPSPs. Bars are means \pm SEM ($n = 6$ Rac3^{KO} and 7 double KO neurons). (C) Perfusion with 100- μ M 4-AP induced ictal discharges in 5 of 6 pyramidal neurons from double KO mice (bottom). No ictal activity was observed in 6 pyramidal neurons from Rac3^{KO} mice (upper). (D and E) Quantification of the effects of 100- and 500- μ M 4-AP on the presence of ictal activity (IA), afterdischarges (ADs); time-to-ictal event (TTI), and IA duration ($n = 6$ cells per genotype for 100 μ M 4-AP; $n = 9$ and 5 Rac3^{KO} and double KO neurons, respectively, for 500 μ M 4-AP). * $P < 0.05$.

whereas the duration of the ictal activity was similar (Fig. 6E). Moreover, in double KO neurons, the TTI measured with 500- μ M 4-AP was shorter than with 100- μ M 4-AP (Fig. 6E).

Synaptic GABAergic inputs induce spontaneous IPSCs in principal glutamatergic cells. The instantaneous frequency of spontaneous IPSCs from CA1 pyramidal neurons recorded in the presence of glutamatergic synapse blockers NBQX and CPP were strongly decreased in double KO compared with Rac3^{KO} (Fig. 7A, B), while the amplitude of IPSCs was similar (Fig. 7C). The frequency of spontaneous IPSCs was decreased also in CA3 pyramidal cells of double KO mice (Supplementary Fig. S7). These results nicely fit with the reduced GABAergic input detected morphologically (Fig. 3), and indicate that the input of GABAergic interneurons to pyramidal neurons is clearly affected in double KO mice.

We found similar effects in the somatosensory cortex, where the analysis in pyramidal neurons from layer V

revealed a decrease in the frequency of spontaneous IPSCs in double KO mice (Fig. 7D, E), while the amplitude of IPSCs was not affected (Fig. 7F). These findings correlate with the increased sensitivity to epileptogenic stimuli recorded in the principal cells of double KO mice, and suggest that the epileptic phenotype observed in these animals is due to the reduced number of interneurons and the consequent reduction of synaptic inhibitory inputs by these cells.

Discussion

We have addressed the role of the Rac1 and Rac3 GTPases during GABAergic interneuron development and shown that these proteins contribute importantly and synergistically to the late stages of cortical and hippocampal interneuron development. We characterized the effects of Rac depletion on the electrophysiological properties of hippocampal neurons,

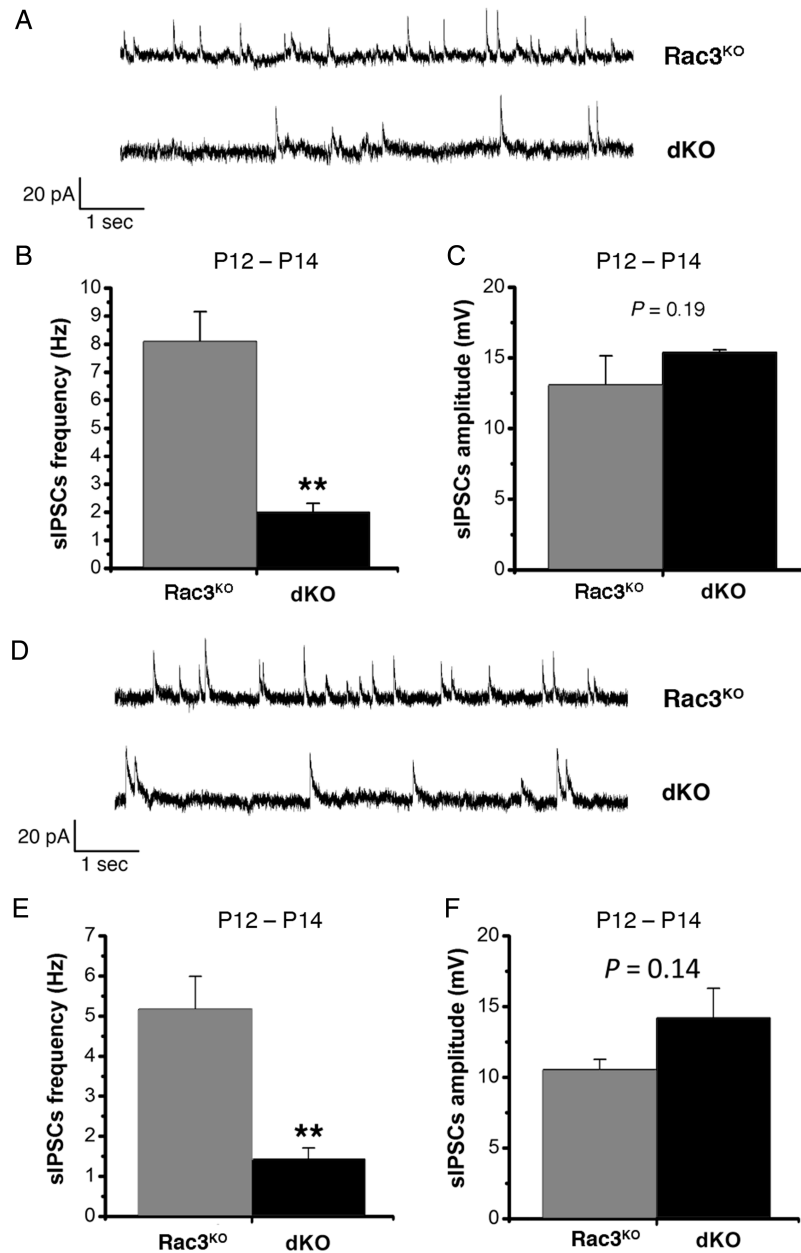


Figure 7. Comparative analysis of spontaneous inhibitory synaptic events in hippocampal CA1 and cortical pyramidal cells. (A–C) Analysis in CA1 hippocampal neurons. (A) Spontaneous IPSCs recorded in CA1 pyramidal cells of *Rac3*^{KO} and double KO mice. (B) Instantaneous frequency of spontaneous IPSCs is significantly decreased in double KO cells ($n = 9$) compared with *Rac3*^{KO} cells ($n = 6$). (C) The amplitude of spontaneous IPSCs is similar in *Rac3*^{KO} and double KO neurons. (D–F) Analysis in cortical neurons. (D) Examples of spontaneous IPSCs recorded in pyramidal neurons from layer V of the somatosensory cortex of *Rac3*^{KO} (upper trace) and double KO mice (lower trace). (E) The instantaneous frequency of spontaneous IPSCs is significantly decreased in double KO somatosensory pyramidal cells ($n = 9$) compared with *Rac3*^{KO} cells ($n = 8$). (F) The amplitude of spontaneous IPSCs is similar in *Rac3*^{KO} and double KO pyramidal neurons. ****** $P < 0.005$.

showing that ablation of the 2 Racs prevents formation of normal inhibitory synapses, likely accounting for the hyperexcitability of the hippocampal neurons.

In previous studies, the conditional deletion of *Rac1* during earlier neural development (*Rac1*^{flox/flox}; *Foxg1*^{Cre/+}) affects brain development, although *Rac1* deletion in the SVZ of MGE and lateral ganglionic eminence (*Rac1*/*Dlx5/6*-CIE) produced no obvious defects in tangential migration (Chen et al. 2007). Indeed, at P12, control and *Rac1*/*Dlx5/6*-CIE mice showed similar number and distribution of PV-positive cortical interneurons, prompting the authors to conclude that *Rac1* is dispensable for the migration of MGE-derived

interneurons per se, although it is required to confer migratory competence on differentiating progenitors. Similar results can be drawn by a more recent study addressing the role of *Rac1* on interneuron progenitors originating in the MGE (Vidaki et al. 2012). In this study, *Rac1* ablation in post-mitotic GABAergic progenitors did not affect interneuron numbers in the cortex, whereas earlier deletion of *Rac1* in *Nkx2.1*-positive proliferating progenitors in the MGE resulted in the reduced number of MGE-derived interneurons in the cortex as a consequence of a defect in the cell cycle exit. These studies show that the conditional deletion of *Rac1* impairs early phases of interneuron differentiation, while the

migration of cortical interneurons per se is not affected if *Rac1* is deleted after progenitors have left the MGE to migrate into the pallium.

On the other hand, we demonstrated that *Rac1* and *Rac3* are both essential for neuronal differentiation and brain development (Corbetta et al. 2009). Unlike single *Rac1* and *Rac3* null mice, double KO mice develop spontaneous epilepsy during postnatal development. These mice feature a dramatic reduction in the number of GABAergic interneurons, mainly PV-positive cells, in the cortex and hippocampus of double KO mice. The comparative analysis between P13 double KO, single KO, and wild-type mice has shown that although single Rac deletion results in a mild loss of cortical/hippocampal PV-positive interneurons, this defect is dramatically more evident in the cortex and hippocampus of double mutant mice, showing that both Rac GTPases contribute synergistically to the development of these cells. The lack of PV-positive neurons in the cortex and hippocampus of double KO mice correlates with the actual decrease of Lhx6-positive interneurons in these mice, indicating that the loss of PV signal is not just due to a defect in PV expression in the interneurons.

Synapsin-I expression is detectable at midgestation with a peak around P20 (Hoesche et al. 1993). Thus, the SynI-Cre prevents early deletion of *Rac1* in MGE-born precursors, as observed with earlier *Rac1* deletion (Chen et al. 2007), and allows late embryonic/postnatal analysis of migratory cells, when *Rac3* is expressed (Corbetta et al. 2005). We can exclude a major effect of *Rac1* depletion on the replication of progenitors and on the precursors in the MGE, because the SynI-Cre was not active in most of the cells in the MGE (Supplementary Fig. S4). The sharp decrease in interneuron numbers could be either due to the loss of these cells after they have reached the final location, and/or to a defect in migration preventing them from reaching their final location. A recent study has shown the increase in hippocampal interneurons between E14.5 and E18, followed by a dramatic decrease after P0, with neuronal death proposed as a potential factor involved (Tricoire et al. 2011). Here, the finding of decreased numbers of CB-positive neurons along the SVZ pathway and the altered morphology of CB-positive precursors in the CP of double KO mice (Fig. 5) indicate that the loss of cortical and hippocampal interneurons may be due to a defect in tangential and radial migration.

Tangential migration occurs via the cortical IZ and MZ for early-born neurons (E11.5–E14.5) and via the cortical SVZ for those born at E14.5–E16.5 (Anderson et al. 2001; Hernández-Miranda et al. 2010). We found no difference between control and double KO cortex in the number of CB-positive cells in the MZ, the migratory route followed by early-born interneurons. Conversely, we found a significant decrease of CB-positive cells along the SVZ route (Fig. 5). One hypothesis is that the CB-positive interneurons present in the MZ of P0 double KO mice have arrived there before the complete inactivation of *Rac1* by the SynI-Cre. On the other hand, the double deletion of *Rac1* and *Rac3* has an effect on the subsequent radial migration of these neurons that show altered morphology. We found that cell death does not increase but remains absent or very low in double KO mice at stages when interneuron migration occurs (Supplementary Fig. S3). Moreover, an evident accumulation of CB-positive precursors along the migratory pathway as a consequence of migratory defects

has not been detected by us. An evident accumulation of CB-positive precursors along the migratory pathway may be hard to detect though. In fact, the strong reduction of PV-positive cells observed in double KO mice is expected to correspond to a moderate reduction of the total CB-positive population of migrating precursors that include also other types of interneurons. We expect that future studies with time-lapse analysis of migrating precursors may help clarifying whether the observed defect following Rac depletion is due to the impairment of the motility of specific types of interneurons.

The finding that simultaneous disruption of *Rac1* and *Rac3* in postmitotic neurons strongly affects the localization of PV-positive MGE-derived interneurons compared with *Rac1^N* or *Rac3^{KO}* mice, in which milder defects were detected, suggests the requirement for the synergistic effects of *Rac1* and *Rac3* GTPases in the mechanisms of tangential and radial migration of these interneurons. The mechanisms determining the strong effects of Rac depletion on the PV-positive interneurons compared with other types of interneurons remain to be established. Different hypotheses may be tested, including the expression of different sets of GTPases and/or their regulators/effectors in different types of interneurons (Cobos et al. 2007); or the different embryonic origin and/or time of generation of distinct populations of interneurons (Tricoire et al. 2011), even within the same ganglionic eminence (Flames et al. 2007; Fogarty et al. 2007; Wonders et al. 2008).

Abnormalities in PV-positive GABAergic interneurons may underlie both an epileptic phenotype (Velíšek et al. 2011), and altered cognition in schizophrenia and autism (Lewis et al. 2005; Orekhova et al. 2007). These may be considered circuitry diseases resulting from uncontrolled neuronal firing and linked to the loss or altered function of inhibitory GABAergic cells (Marín 2012). Our work contributes to the identification of the intracellular mechanisms that may underlie these diseases. Much work remains to clarify the links of Rac GTPases to upstream signals and downstream targets required for interneuron maturation.

Supplementary Material

Supplementary material can be found at: <http://www.cercor.oxfordjournals.org/>.

Funding

This work was supported by Telethon–Italy (grants GGP09078 and GGP12126), Regione Lombardia (ID SAL-58, grant number 16695), MIUR (grant 20082RPFYF), and Fondazione Italiana Sclerosi Multipla (grant number 2010/R/14). Funding to pay the Open Access publication charges for this article was provided by Telethon – Italy.

Notes

We thank Jamey Marth (University of California, San Diego) for SynI-Cre mice, Victor Tybulewicz (MRC, London) for the *Rac1^{flox/flox}* mice, Vassilis Pachnis (MRC, London) for the probe for Lhx6, Cesare Covino of the Alembic facility for technical help, Gaia Colasante, Alessandro Sessa and Vania Broccoli (San Raffaele Scientific Institute, Milano) for helpful discussion and for sharing reagents. *Conflict of Interest:* None declared.

References

- Albertinazzi C, Gilardelli D, Paris S, Longhi R, de Curtis I. 1998. Overexpression of a neural-specific rho family GTPase, cRac1B, selectively induces enhanced neurogenesis and neurite branching in primary neurons. *J Cell Biol.* 142:815–825.
- Albertinazzi C, Za L, Paris S, de Curtis I. 2003. ADP-ribosylation factor 6 and a functional PIX/p95-APP1 complex are required for Rac1B-mediated neurite outgrowth. *Mol Biol Cell.* 14:1295–1307.
- Alcantara S, de Lecea L, Del Rio JA, Ferrer I, Soriano E. 1996. Transient colocalization of parvalbumin and calbindin D28k in the postnatal cerebral cortex: evidence for a phenotypic shift in developing nonpyramidal neurons. *Eur J Neurosci.* 8:1329–1339.
- Anderson SA, Eisenstat DD, Shi L, Rubenstein JL. 1997. Interneuron migration from basal forebrain to neocortex: dependence on Dlx genes. *Science.* 278:474–476.
- Anderson SA, Marín O, Horn C, Jennings K, Rubenstein JL. 2001. Distinct cortical migrations from the medial and lateral ganglionic eminences. *Development.* 128:353–363.
- Ang ES Jr, Haydar TF, Gluncic V, Rakic P. 2003. Four-dimensional migratory coordinates of GABAergic interneurons in the developing mouse cortex. *J Neurosci.* 23:5805–5815.
- Batista-Brito R, Fishell G. 2009. The developmental integration of cortical interneurons into a functional network. *Curr Top Dev Biol.* 87:81–118.
- Bolis A, Corbetta S, Cioce A, de Curtis I. 2003. Differential distribution of Rac1 and Rac3 GTPases in the developing mouse brain: implications for a role of Rac3 in Purkinje cell differentiation. *Eur J Neurosci.* 18:2417–2424.
- Brooks-Kayal A. 2011. Molecular mechanisms of cognitive and behavioral comorbidities of epilepsy in children. *Epilepsia.* 52(Suppl. 1):13–20.
- Chen L, Liao G, Waclaw RR, Burns KA, Linnquist D, Campbell K, Zheng Y, Kuan CY. 2007. Rac1 controls the formation of midline commissures and the competency of tangential migration in ventral telencephalic neurons. *J Neurosci.* 27:3884–3893.
- Cobos I, Borello U, Rubenstein JL. 2007. Dlx transcription factors promote migration through repression of axon and dendrite growth. *Neuron.* 54:873–888.
- Cobos I, Calcagnotto ME, Vilaythong AJ, Thwin MT, Noebels JL, Baraban SC, Rubenstein JL. 2005. Mice lacking Dlx1 show subtype-specific loss of interneurons, reduced inhibition and epilepsy. *Nat Neurosci.* 8:1059–1068.
- Corbetta S, Gualdoni S, Albertinazzi C, Paris S, Croci L, Consalez GG, de Curtis I. 2005. Generation and characterization of Rac3 knockout mice. *Mol Cell Biol.* 25:5763–5776.
- Corbetta S, Gualdoni S, Ciceri G, Monari M, Zuccaro E, Tybulewicz VL, de Curtis I. 2009. Essential role of Rac1 and Rac3 GTPases in neuronal development. *FASEB J.* 23:1347–1357.
- Danglot L, Triller A, Marty S. 2006. The development of hippocampal interneurons in rodents. *Hippocampus.* 16:1032–1060.
- de Curtis I. 2008. Functions of Rac GTPases during neuronal development. *Dev Neurosci.* 30:47–58.
- Flames N, Pla R, Gelman DM, Rubenstein JLR, Puelles L, Marín O. 2007. Delineation of multiple subpallial progenitor domains by the combinatorial expression of transcriptional codes. *J Neurosci.* 27:9682–9695.
- Fogarty M, Grist M, Gelman D, Marín O, Pachnis V, Kessaris N. 2007. Spatial genetic patterning of the embryonic neuroepithelium generates GABAergic interneuron diversity in the adult cortex. *J Neurosci.* 27:10935–10946.
- Gelman DM, Marín O. 2010. Generation of interneuron diversity in the mouse cerebral cortex. *Eur J Neurosci.* 31:2136–2141.
- Grigoriou M, Tucker AS, Sharpe PT, Pachnis V. 1998. Expression and regulation of Lhx6 and Lhx7, a novel subfamily of LIM homeodomain encoding genes, suggests a role in mammalian head development. *Development.* 125:2063–2074.
- Haataja L, Groffen J, Heisterkamp N. 1997. Characterization of RAC3, a novel member of the Rho family. *J Biol Chem.* 272:20384–20388.
- Hernández-Miranda LR, Parnavelas JG, Chiara F. 2010. Molecules and mechanisms involved in the generation and migration of cortical interneurons. *ASN Neuro.* 2:e00031.
- Hevner RF, Daza RA, Englund C, Kohtz J, Fink A. 2004. Postnatal shifts of interneuron position in the neocortex of normal and reeler mice: evidence for inward radial migration. *Neuroscience.* 124:605–618.
- Hoesche C, Sauerwald A, Veh RW, Krippel B, Kilimann MW. 1993. The 5'-flanking region of the rat synapsin I gene directs neuron-specific and developmentally regulated reporter gene expression in transgenic mice. *J Biol Chem.* 268:26494–26502.
- Inan M, Welagen J, Anderson SA. 2012. Spatial and temporal bias in the mitotic origins of somatostatin- and parvalbumin-expressing interneuron subgroups and the chandelier subtype in the medial ganglionic eminence. *Cereb Cortex.* 22:820–827.
- Lewis DA, Hashimoto T, Volk DW. 2005. Cortical inhibitory neurons and schizophrenia. *Nat Rev Neurosci.* 6:312–324.
- Malosio ML, Gilardelli D, Paris S, Albertinazzi C, de Curtis I. 1997. Differential expression of distinct members of Rho family GTP-binding proteins during neuronal development: identification of Rac1B, a new neural-specific member of the family. *J Neurosci.* 17:6717–6728.
- Marín O. 2012. Interneuron dysfunction in psychiatric disorders. *Nat Rev Neurosci.* 13:107–120.
- Martini FJ, Valiente M, López-Bendito G, Szabó G, Moya F, Valdeolillos M, Marín O. 2009. Biased selection of leading process branches mediates chemotaxis during tangential neuronal migration. *Development.* 136:41–50.
- Miyoshi G, Hjerling-Leffler J, Karayannis T, Sousa VH, Butt SJ, Battiste J, Johnson JE, Machold RP, Fishell G. 2010. Genetic fate mapping reveals that the caudal ganglionic eminence produces a large and diverse population of superficial cortical interneurons. *J Neurosci.* 30:1582–1594.
- Nadarajah B, Alifragis P, Wong RO, Parnavelas JG. 2002. Ventricle-directed migration in the developing cerebral cortex. *Nat Neurosci.* 5:218–224.
- Orekhova EV, Stroganova TA, Nygren G, Tsetlin MM, Posikera IN, Gillberg C, Elam M. 2007. Excess of high frequency electroencephalogram oscillations in boys with autism. *Biol Psychiatry.* 62:1022–1029.
- Pennucci R, Tavano S, Tonoli D, Gualdoni S, de Curtis I. 2011. Rac1 and Rac3 GTPases regulate the development of hilar mossy cells by affecting the migration of their precursors to the hilus. *PLoS One.* 6:e24819.
- Pla R, Borrell V, Flames N, Marín O. 2006. Layer acquisition by cortical GABAergic interneurons is independent of Reelin signaling. *J Neurosci.* 26:6924–6934.
- Schaeren-Wiemers N, Gerfin-Moser A. 1993. A single protocol to detect transcripts of various types and expression levels in neural tissue and cultured cells: in situ hybridization using digoxigenin-labelled cRNA probes. *Histochemistry.* 100:431–440.
- Soriano P. 1999. Generalized lacZ expression with the ROSA26 Cre reporter strain. *Nat Genet.* 21:70–71.
- Stoop R, Pralong E. 2000. Functional connections and epileptic spread between hippocampus, entorhinal cortex and amygdala in a modified horizontal slice preparation of the rat brain. *Eur J Neurosci.* 12:3651–3663.
- Stühmer T, Puelles L, Ekker M, Rubenstein JL. 2002. Expression from a Dlx Gene Enhancer Marks Adult Mouse Cortical GABAergic neurons. *Cereb Cortex.* 12:75–85.
- Tanaka DH, Maekawa K, Yanagawa Y, Obata K, Murakami F. 2006. Multidirectional and multizonal tangential migration of GABAergic interneurons in the developing cerebral cortex. *Development.* 133:2167–2176.
- Tanaka DH, Nakajima K. 2012. Migratory pathways of GABAergic interneurons when they enter the neocortex. *Eur J Neurosci.* 35:1655–1660.
- Tricoire L, Pelkey KA, Erkkila BE, Jeffries BW, Yuan X, McBain CJ. 2011. A blueprint for the spatiotemporal origins of mouse hippocampal interneuron diversity. *J Neurosci.* 31:10948–10970.
- Tyzio R, Ivanov A, Bernard C, Holmes GL, Ben-Ari Y, Khazipov R. 2003. Membrane potential of CA3 hippocampal pyramidal cells during postnatal development. *J Neurophysiol.* 90:2964–2972.
- Velišek L, Shang E, Velišková J, Chachua T, Macchiarulo S, Maglakelidze G, Wolgemuth DJ, Greenberg DA. 2011. GABAergic neuron deficit as

- an idiopathic generalized epilepsy mechanism: the role of BRD2 haploinsufficiency in juvenile myoclonic epilepsy. *PLoS One*. 6:e23656.
- Vidaki M, Tivodar S, Doulgeraki K, Tybulewicz V, Kessaris N, Pachnis V, Karagogeos D. 2012. Rac1-dependent cell cycle exit of MGE precursors and GABAergic interneuron migration to the cortex. *Cereb Cortex*. 22:680–692.
- Walmsley MJ, Ooi SK, Reynolds LF, Smith SH, Ruf S, Mathiot A, Vanes L, Williams DA, Cancro MP, Tybulewicz VL. 2003. Critical roles for Rac1 and Rac2 GTPases in B cell development and signaling. *Science*. 302:459–462.
- Wonders CP, Anderson SA. 2006. The origin and specification of cortical interneurons. *Nat Rev Neurosci*. 7:687–696.
- Wonders CP, Taylor L, Welagen J, Mbata IC, Xiang JZ, Anderson SA. 2008. A spatial bias for the origins of interneuron subgroups within the medial ganglionic eminence. *Dev Biol*. 314:127–136.
- Zhao Y, Flandin P, Long JE, Cuesta MD, Westphal H, Rubenstein JL. 2008. Distinct molecular pathways for development of telencephalic interneuron subtypes revealed through analysis of Lhx6 mutants. *J Comp Neurol*. 510:79–99.
- Zhu Y, Romero MI, Ghosh P, Ye Z, Charnay P, Rushing EJ, Marth JD, Parada LF. 2001. Ablation of NF1 function in neurons induces abnormal development of cerebral cortex and reactive gliosis in the brain. *Genes Dev*. 15:859–876.